Structure and properties of suction-cast Pr-(Fe, Co)-(Zr, Nb)-B rod magnets

K. Pawlik[1]

[1] Department of Physics, Częstochowa University of Technology, Al. Armii Krajowej 19, 42-200 Częstochowa, Poland

Abstract

The rod specimens were produced from $Pr_9Fe_{50+x}Co_{13}Zr_1Nb_4B_{23-x}$ (x=0, 5, 8) alloys using the suction-casting technique. Subsequent devitrification annealing of those samples resulted in the change of their phase structure and magnetic properties. For annealed specimens of all investigated compositions, the Mössbauer spectroscopy as well as Rietveld analyses of X-ray diffractions have shown a presence of two crystalline phases: the hard magnetic $Pr_2Fe_{11.2}Co_{2.8}B$ and paramagnetic $Pr_{1+x}Fe_4B_4$, which have precipitated within the amorphous matrix. These techniques allowed to determine the weight fractions of constituent phases. Furthermore, the microstructural changes with the alloy composition were observed.

Magnetic measurements of annealed rods, allowed to calculate the switching field distributions (SFD) and δM plots in order to determine the strength and character of magnetic interactions between grains of constituent phases. Furthermore, the magnetic measurements of minor hysteresis loops at various temperatures allowed to characterize the magnetization reversal processes present in annealed rods.

Samples preparation

The alloys of nominal compositions $Pr_9Fe_{50+x}Co_{13}Zr_1Nb_4B_{23-x}$ (x = 0, 5, 8) were produced by the arc-melting technique.

Rapidly solidified 1 mm diameter rods were produced by suction-casting.

The annealing was carried out at 983 K for 5 min in order to obtain the nanocrystalline microstructure and induce hard magnetic properties.

Experimental methods

The phase constitution was determined using X-ray diffractometry (XRD). The XRD scans were measured using Bruker D8 Advanced diffractometer equipped with Cu tube. The phase constitution of the annealed samples was analyzed using Rietveld refinement of the X-ray diffraction spectra. In order to quantify the amorphous and crystalline phases the PONKCS (Partial Or No Known Crystal Structure) method was applied.

The microstructure was examined by transmission electron microscopy (TEM). Magnetic properties of the ribbons were measured by LakeShore VSM magnetometer operating in an external magnetic field up to 2T.

Results

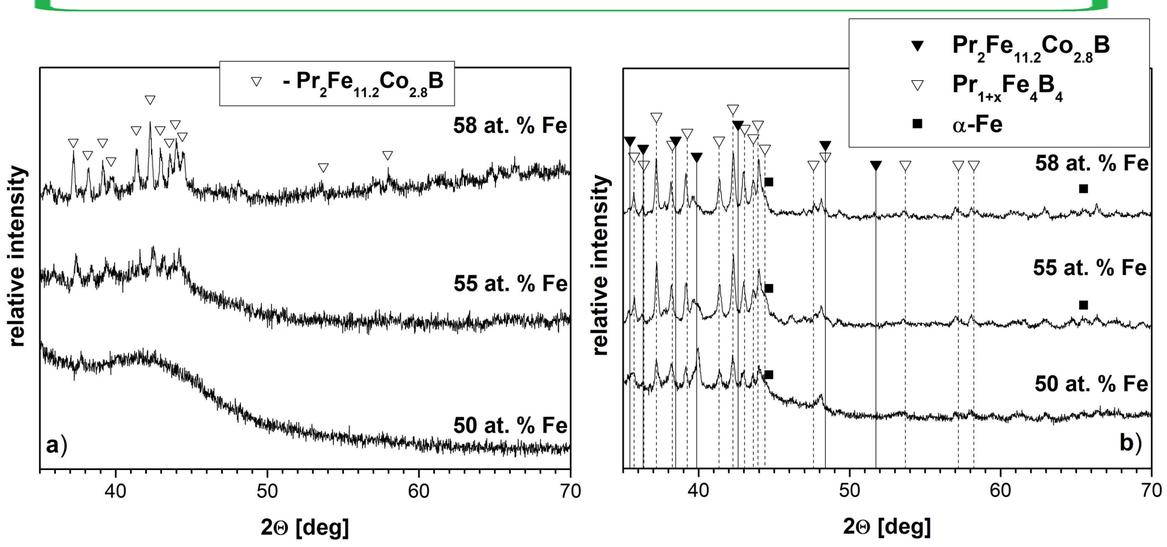

Fig.1. XRD patterns measured for 1 mm diameter rods of $Pr_9Fe_{50+x}Co_{13}Zr_1Nb_4B_{23-x}$ alloys in the as-cast state (a) and subjected to annealing at 983 K for 5 min (b).

Table 1. Rietveld refinement results; refined cell parameters (a, c), crystallite sizes (d) and weight fraction (wf) of crystalline phases (2:14:1 - $Pr_2Fe_{11.2}Co_{2.8}B$; 1:4:4 - $Pr_{1+x}Fe_4B_4$; α-Fe) and amorphous phase.

at. % of Fe	phase	a [nm]	c [nm]	d [nm]	wf [%]
50 (annealed)	2:14:1	0.8774 ± 0.0001	1.2149 ± 0.0002	35.0 ± 0.6	56.3 ± 0.7
	1:4:4	0.7099 ± 0.0001	3.4942 ± 0.0012	17.3 ± 0.6	36.6 ± 0,6
	α-Fe	0.2868 ± 0.0001	-	10.1 ± 0.5	7.1 ± 0.3
55 (as-cast)	2:14:1	0.8811 ± 0.0001	1.2247 ± 0.0002	31.1 ± 1.1	33.6 ± 0.6
	1:4:4	0.7164 ± 0.0002	3.5073 ± 0.0011	14.4 ± 0.8	15.3 ± 0.4
	amorphous	-	-	-	51.1 ± 0.7
55 (annealed)	2:14:1	0.8774 ± 0.0001	1.2171 ± 0.0002	55.1 ± 0.9	38.9 ± 0.7
	1:4:4	0.7107 ± 0.0001	3.4820 ± 0.0010	25.3 ± 0.9	49.4 ± 0.7
	α-Fe	0.2873 ± 0.0001	-	8.7 ± 05	11.7 ± 0.4
58 (as-cast)	2:14:1	0.8799 ± 0.0001	1.2241 ± 0.0002	55.7 ± 1.2	25.5 ± 0.6
	1:4:4	0.7128 ± 0.0001	3.4918 ± 0.0012	21.4 ± 0.7	23.7 ± 0.6
	amorphous	-	-	-	50.8 ± 0.7
58 (annealed)	2:14:1	0.8756 ± 0.0001	1.2150 ± 0.0002	97.6 ± 1.7	39.7 ± 0.7
	1:4:4	0.7084 ± 0.0001	3.4784 ± 0.0012	33.1 ± 1.2	45.5 ± 0.7
	α-Fe	0.2867 ± 0.0001	-	12.3 ± 0.5	14.8 ± 0.4

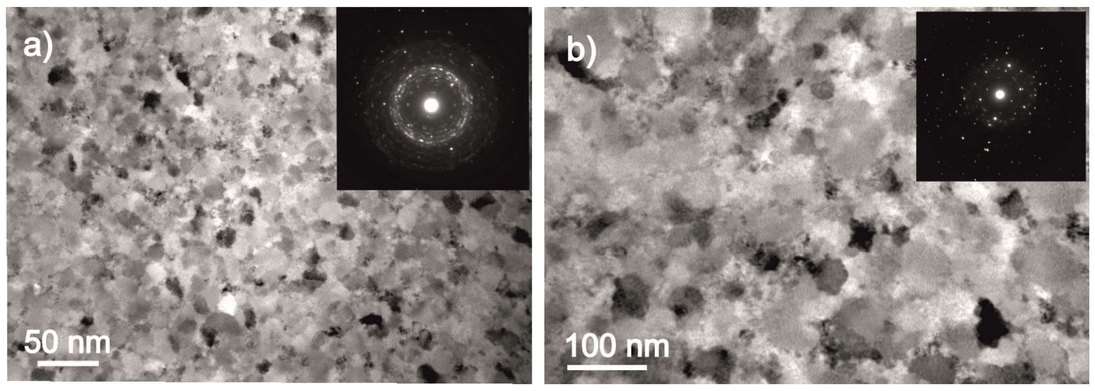

Fig.2. Transmission electron microscopy images obtained for the annealed 1 mm diameter rods of the $Pr_9Fe_{50}Co_{13}Zr_1Nb_4B_{23}$ (a) and $Pr_9Fe_{58}Co_{13}Zr_1Nb_4B_{15}$ (b) alloys.

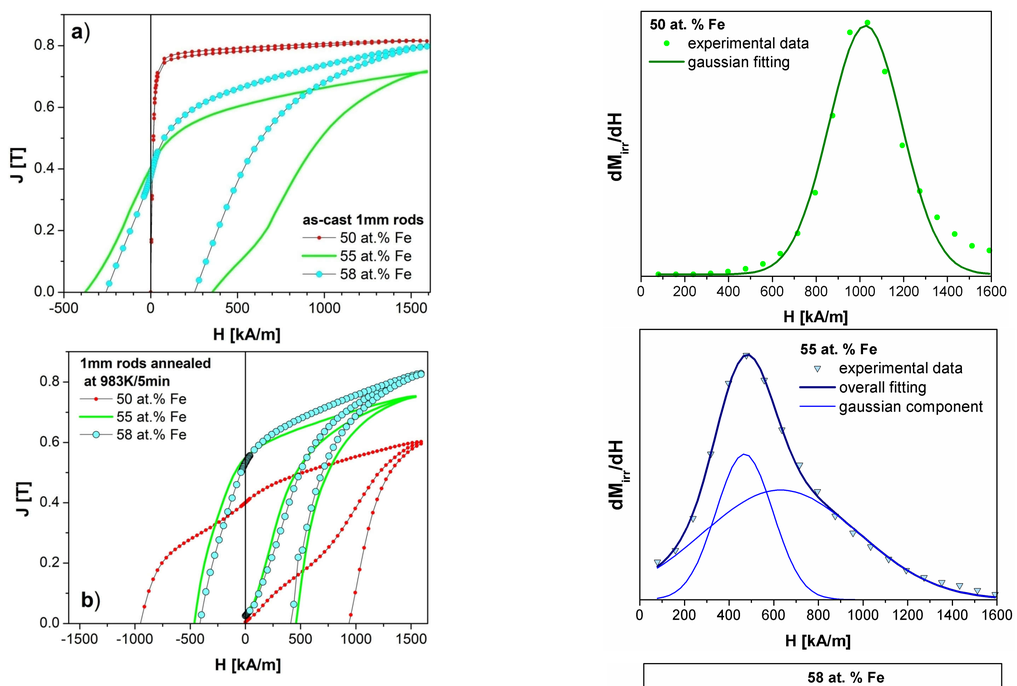

Fig.3. The hysteresis loops measured for 1 mm diameter rods of $Pr_9Fe_{50+x}Co_{13}Zr_1Nb_4B_{23-x}$ alloys in the as-cast state (a) and after annealing at 983 K for 5 min (b).

Fig.5. The switching field distributions (SDF) for the annealed 1 mm diameter rods of the $Pr_9Fe_{50+x}Co_{13}Zr_1Nb_4B_{23-x}$ (x = 0, 5, 8) alloys.

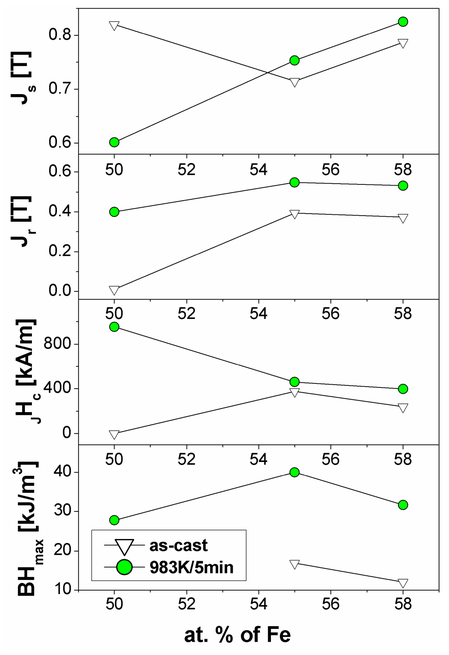

Fig.4. Dependences of the saturation polarization J_s, remanence J_r, coercivity field ${}_JH_c$ and maximum energy product $(BH)_{max}$ on the alloy composition measured for 1mm dia. Rods in as-cast state and after annealing at 983 K for 5 min.

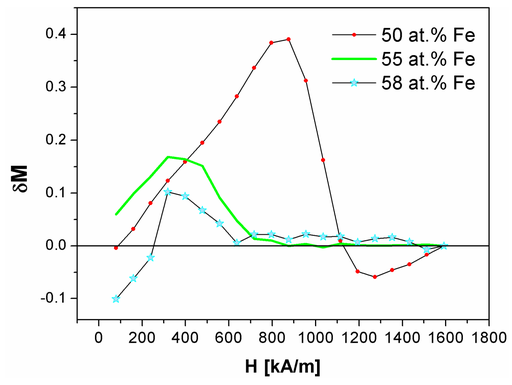

Fig.6. The dM plots for the annealed 1 mm diameter rods of the $Pr_9Fe_{50+x}Co_{13}Zr_1Nb_4B_{23-x}$ (x = 0, 5, 8) alloys.

Conclusions

It was shown by XRD studies that glass forming ability of $Pr_9Fe_{50+x}Co_{13}Zr_1Nb_4B_{23-x}$ (x = 0, 5, 8) alloys decreases with increase of the Fe content. The x=0 alloy rod samples in the as-cast state were fully amorphous, while higher Fe content resulted in precipitation of the hard magnetic $Pr_2Fe_{11.8}Co_{2.8}B$ and paramagnetic $Pr_{1+x}Fe_4B_4$ phases within the amorphous matrix. The phase constitution of the as-cast samples undoubtedly affected the final composition and magnetic properties of samples subjected to annealing. Initial state of rods also influenced the microstructure of annealed specimens. Heat treatment of fully amorphous rods of the x=0 alloy resulted in formation of homogenous microstructure consisting of nanocrystals of diameters between 10-20 nm. This fact and large fraction of the hard magnetic phase resulted in the highest coercivity of this alloy rods. Partial crystallization of as-cast rods of higher Fe contents caused formation of heterogeneous microstructure during annealing. However, the highest J_r and $(BH)_{max}$ was achieved for annealed rods of $Pr_9Fe_{55}Co_{13}Zr_1Nb_4B_{18}$ alloy, which might be related to the presence of the α-Fe phase of the large saturation polarization. Relatively low crystallite sizes of this soft magnetic phase may contribute to the exchange spring effect in these hard magnetic materials. It was shown that the increase of B content (at expense of Fe) in the chemical composition of the alloy promoted formation of paramagnetic phase during annealing. Furthermore, higher B to Fe ratio together with Zr and Nb additions hindered the crystal growth. Broad switching field distributions reflecting wide range of magnetic fields that cause the magnetization reversal are related to heterogeneity of the microstructure. The *δM* plots have shown that the strongest exchange interactions between grains occur for annealed rods of the x=0 alloy with the finest crystallites. For samples with coarser crystallites existence of multi domain structure and dipolar interactions causes reduction of *δM* values.